XAFS Studies of Soft-Heavy-Metal-Ion-Intercalated M_xMoS_2 ($M = Hg^{2+}$, Ag^+) Solids

Patrick G. Allen

Seaborg Institute for Transactinium Science, Lawrence Livermore National Laboratory, Livermore, California 94550

Alexander E. Gash,† Peter K. Dorhout,*,‡ and Steven H. Strauss*

Department of Chemistry, Colorado State University, Fort Collins, Colorado 80523

Received May 11, 2000. Revised Manuscript Received April 10, 2001

XAFS studies were performed on two new soft-heavy-metal-ion-intercalated materials M_x-MoS_2 ($M = Hg^{2+}$, Ag^+). For the compound $Hg_{0.32}MoS_2$, EXAFS results show an average Hg coordination environment consisting of ≈2 S atoms at 2.38 Å and ≈0.2 (±35%) Hg atoms at 2.55 Å. Along with Hg XANES analysis, these data indicate that the Hg atoms in this compound are present as a mixture of mercuric and mercurous ions. Ag EXAFS analysis of the compound $Ag_{0.61}MoS_2$ indicates a Ag coordination environment consisting of ≈2 S atoms at 2.43 Å. Ag EXAFS and XANES results for heat-treated $Ag_{0.61}MoS_2$ indicate that the Ag coordination environment has changed to that nearly identical for silver metal with several Ag−Ag interactions detected. The results suggest that heat treatment of $Ag_{0.61}MoS_2$ facilitates the chemical reduction of the intercalated silver ions to elemental silver. In addition, Mo EXAFS and XANES analyses indicate that both the Hg- and Ag-intercalated compounds have significant amounts of the 1T-phase of MoS_2 in them. Prolonged exposure of both of these materials to an aerobic atmosphere does not affect their Mo EXAFS. Comparison of these results with those for exfoliated and restacked MoS_2 suggests that different intercalated guest ions afford different oxidative stabilities to the host MoS_2 layers. This hypothesis is used to rationalize some inconsistencies in previous reports of M_xMoS_2 XAFS studies.

Introduction

There are numerous reports on the synthesis, characterization, and physicochemical properties of polymer,[1,2] metal-ion-,[3,4] metal-chalcogenide-cluster-,[5] metal-oxide-cluster-,[6] and metallocene-intercalated molybdenum disulfide (MoS_2).[7] All these materials were synthesized using the well-known method of exfoliation and flocculation of Li_xMoS_2 reported by Gee et al. (see (1)).[8] The colloid created in (1) can be induced to flocculate into a solid by the addition of cationic species to the solution or by a change in pH. Many researchers believe that the MoS_2 in the above colloid exists as negatively charged $[MoS_2]^{n-}$ slabs. This has been inferred from the intercalation of cationic guests yielding a charge balance within the solid. Although there has been active research in this area for the past 14 years, there are still fundamental questions about the mechanism of guest inclusion into MoS_2. Although many of these questions were posed in the seminal papers, the authors have left the questions to speculation and have proven little through additional experimentation. Many of these materials have potential applications as heterogeneous catalysis,[9−11] superconductors,[12,13] ionic or electronic conductors,[14,15] or reversible battery electrodes.[16−18] We are currently investigating a new application of these

$$Li_xMoS_2(s) + yH_2O \rightarrow Li_{(x-y)}MoS_2(col) + y/2H_2(g) + yOH^-(aq) + yLi^+(aq) \quad (1)$$

* To whom correspondence should be addressed. E-mail: pkd@LAMAR.colostate.edu; strauss@mail.chm.colostate.edu.

† Presently at Chemistry and Materials Science Division, Lawrence Livermore National Laboratory, Livermore, CA 94550.

‡ P.K.D. is an A. P. Sloan Fellow and Camille Dreyfus Teacher Scholar.

(1) Bissessur, R.; Kanatzidis, M. G.; Schindler, J. L.; Kannewurf, C. R. *J. Chem. Soc., Chem. Commun.* **1993**, 1582.

(2) Wang, L.; Schindler, J.; Thomas Albritton, J.; Kannewurf, C. R.; Kanatzidis, M. *Chem. Mater.* **1995**, *7*, 1753.

(3) Golub, A. S.; Protozenko, G. A.; Yanovskaya, I. M.; Lependina, O. L.; Novikov, Y. N. *Mendeleev Commun.* **1993**, 199.

(4) Dungey, K. E.; Curtis, M. D.; Penner-Hahn, J. E. *Chem. Mater.* **1998**, *10*, 2152.

(5) Bissessur, R.; Heising, J.; Hirpo, W.; Kanatzidis, M. *Chem. Mater.* **1996**, *8*, 318.

(6) Heising, J.; Bonhomme, F.; Kanatzidis, M. G. *J. Solid State Chem.* **1998**, *139*, 22.

(7) Tagaya, H.; Hashimoto, T.; Karasu, M. *Chem. Lett.* **1991**, 2133.

(8) Gee, M. A.; Frindt, R. F.; Joensen, P.; Morrision, R. S. *Mater. Res. Bull.* **1986**, *21*, 543.

(9) Furimsky, E.; Amberg, C. H. *Can. J. Chem.* **1975**, *53*, 2542.

(10) Miremandi, B. K.; Morrision, S. R. *J. Catal.* **1987**, *103*, 334.

(11) Bockrath, B. C.; Parfitt, D. S. *Catal. Lett.* **1995**, *33*, 201.

(12) Somoano, R. B.; Rembaum, A. *J.P.L. Q. Techn. Rev.* **1971**, *1*, 35.

(13) Somoano, R. B.; Hadek, V.; Rembaum, A. *J.P.L. Q. Techn. Rev.* **1972**, *2*, 83.

(14) Gonzalez, G.; Santa Ana, M. A.; Benavente, E. *J. Chem. Phys. Solids* **1997**, *58*, 1457.

(15) Gonzalez, G.; Santa Ana, M. A.; Benavente, E.; Donoso, J. P.; Bonagamba, T. J.; Mello, N. C.; Panepucci, H. *Solid State Ionics* **1996**, *85*, 225.

(16) Julien, C.; Samaras, I.; Saikh, S. I.; Balkanski, M. *Mater. Res. Soc. Symp. Proc.* **1989**, *135*, 467.

10.1021/cm000389p CCC: $20.00
Published on Web 06/02/2001

materials in another area: waste remediation. We have reported that $Li_{1.3}MoS_2$ is an effective, selective, and redox-recyclable extractant for the removal of Hg(II) from aqueous solution.[19−21] Therefore, for our purposes, we are very interested in the mechanism of ion removal.

There are three possible mechanisms of ion removal that will be specifically addressed in this report. They are as follows: (1) the process is simple ion exchange between the cations in solution and the lithium cations contained within the negatively charged MoS_2 layers; (2) the removal of cations involves the simple adsorption of a counterion with the cationic species (i.e., ion-pair extraction); or (3) Li_xMoS_2 acts as a strong reducing agent that reduces the metal ions to their elemental forms, which consequently precipitate out of solution onto the MoS_2 layers. To completely address the issues discussed above, there is a crucial need for knowledge of both the oxidation states and the coordination environments of the elements that comprise the host material and the guest species. In the absence of a single-crystal X-ray structure, this type of information can be gained through X-ray absorption fine structure (XAFS) spectroscopic methods, which includes the specific techniques of extended XAFS (EXAFS) and X-ray absorption near-edge structure (XANES).

A great deal of useful chemical information can be gained from both polycrystalline and amorphous samples using XAFS analyses.[22] EXAFS can determine the coordination number, neighbor identity, and near-neighbor distances, while XANES measures the effective charge for a desired absorbing atom. Historically, XAFS has been applied to characterize metal sites in biological systems, which are notoriously noncrystalline.[23] More recently, this technique has been successfully applied to characterize both the host and the guest species in metal-included MoS_2 compounds.[4,24,25]

EXAFS analyses have been used to detect the presence of both the 1T- and 2H-phases of MoS_2.[4,24−26] Each phase was found to possess distinct EXAFS Fourier transforms (representing a pseudo-radial distribution function) with sufficiently different Mo−Mo interaction distances that allowed identification of each phase. Curtis and co-workers determined that lithium-intercalated MoS_2 is composed of layers of MoS_2 in the so-called 1T-phase.[4] The 1T-phase displayed a structural distortion from the 2H-phase wherein Mo_3 trimers were modeled. This agglomeration gave rise to two distinct Mo−Mo shell distances of ≈2.8 and ≈3.8 Å that are significantly different from the single Mo−Mo shell distance of 3.16 Å seen in EXAFS transforms of the 2H-phase. They also determined that exfoliated and restacked MoS_2 contains a mixture of both the 1T- and 2H-phases. In addition, the EXAFS analyses of Co^{2+}-intercalated MoS_2 were used to elucidate the coordination environments of both the host (Co^{2+}) and the guest metals (Mo). This study demonstrated that the MoS_2 layers of the Co^{2+}-intercalated host material also had a mixture of both the 1T- and 2H-phases.

EXAFS has proven useful in other studies of metal-included MoS_2 compounds. For example, Zubavichus and co-workers have characterized the coordination environment of the host−guest metals in several metal-included M_yMoS_2 ($M = Co^{2+}$, Mn^{2+}, Ru^{2+}, Ni^{2+}) compounds.[24,25] However, according to these studies, the MoS_2 layers of the Co^{2+}-included material were only present as the 2H-phase. The difference between the results of this study and Curtis' has been attributed to different thermal histories for the two compounds. (Thermal treatment of the 1T-phase induces a transformation back to the 2H-phase.) Interestingly enough, in the Zubavichus et al. study, the Mn^{2+}-included compound displayed Mo EXAFS, indicating only the 2H-phase also. However, both the Ru^{2+}- and Ni^{2+}-included material displayed Mo EXAFS that indicated a mixture of both the 1T- and 2H-phases.

The 1T-phase of MoS_2 has been reportedly observed in exfoliated and restacked MoS_2.[1,27,28] It was also found via a different synthetic route developed by Schöllhorn.[29] More recently, electron diffraction studies have shown the presence of a superstructure in compounds prepared by both methods; however, the superstructures observed were not identical.[30−32] Therefore, it is increasingly likely that both compounds, previously called "1T-MoS_2", have slightly different structures and properties. The difference in the two polytypes resides in the arrangement of the Mo atoms in the layers. In the restacked material, the Mo atoms have shifted relative to 2H−MoS_2 to form zigzag chains of close Mo−Mo contacts (≈2.8 Å). In Schöllhorn's 1T-material, the Mo atoms have shifted relative to 2H−MoS_2 to form close Mo−Mo contacts in Mo_3 trimers. Both of these structural changes lead to a distorted octahedral environment around the Mo atoms and the similarity of the environments in each material likely led to their classification as the same phase. However, in the absence of a classification of a new phase of MoS_2, this report will refer to both of these materials as the "1T-phase". This distinction is made only to indicate that their intralayer atomic arrangement consists of more direct Mo−Mo interactions than that in the 2H-phase.

(17) Julien, C.; Samaras, I.; Mouget, G. *Chemical and Electrochemical Intercalation Techniques*; Balkanski, M., Ed.; Elsevier: Amsterdam, 1991; p 397.
(18) Julien, C. *Lithium Insertion in Chalcogenides: Electrochemical Properties and Electrode Applications*; Balkanski, M., Ed.; Elsevier: Ansterdam, 1991; p 309.
(19) Gash, A. E.; Spain, A. L.; Dysleski, L. M.; Flashenriem, C. J.; Kalaveshi, A.; Dorhout, P. K.; Strauss, S. H. *Environ. Sci. Technol.* **1998**, 1007.
(20) Dorhout, P. K.; Strauss, S. H. *The Design, Synthesis, and Characterization of Redox-Recyclable Materials for Efficient Extraction of Heavy Element Ions from Aqueous Waste Streams*; Winter, C. E., Ed.; American Chemical Society: Washington, D.C., 1999; p 53.
(21) Strauss, S. H. *Redox-Recyclable Extraction and Recovery of Heavy Metal Ions and Radionuclides from Aqueous Media*; Bond, A. H., Dietz, M. L., Rogers, R. D., Eds.; American Chemical Society: Washington, D.C., 1999; p 156.
(22) Drago, R. S. *Physical Methods for Chemists*, 2nd ed.; Saunders College Publishing: Ft. Worth, TX, 1992.
(23) Penner-Hahn, J. E. *Metal Clusters in Biological Systems*; Que, L., Ed.; Amercian Chemical Society: Washington, D.C., 1988.
(24) Zubavichus, Y. V.; Golub, A. S.; Novikov, Y. N.; Slovokhotov, Y. L.; Nesmayanov, A. N.; Schilling, P. J.; Tittsworth, R. C. *J. Phys., IV* **1997**, *7* (C2, X-ray Absorption Fine Structure, Vol. 2), 1057.
(25) Zubavichus, Y. V.; Slovokhotov, Y. L.; Schilling, P.; Tittsworth, R. C.; Golub, A. S.; Protzenko, G. A.; Novikov, Y. N. *Inorg. Chim. Acta* **1998**, *280*, 211.
(26) Joensen, P.; Crozier, E. D.; Alberding, N.; Frindt, R. F. *J. Phys. C: Solid State Phys.* **1987**, *20*, 4043.
(27) Lemmon, J. P.; Lerner, M. M. *Chem. Mater.* **1994**, *6*, 207.
(28) Wypych, F.; Schöllhorn, R. *Quim. Nova* **1996**, 5.
(29) Wypych, F.; Schöllhorn, R. *J. Chem. Soc, Chem. Commun.* **1992**, 1386.
(30) Wypych, F.; Prins, R.; Weber, T. *Surf. Sci.* **1997**, *380*, L474.
(31) Wypych, F.; Weber, T.; Prins, R. *Chem. Mater.* **1998**, *10*, 723.
(32) Heising, J.; Kanatzidis, M. G. *J. Am. Chem. Soc.* **1999**, *121*, 638.

In this paper we report the XAFS characterization of two metal-intercalated compounds of MoS_2 (M_xMoS_2; M = Hg^{2+}, Ag^+).[19,20] According to XAFS analyses, both of these materials exist with a Mo coordination environment that appears to be a combination of both the 1T- and 2H-phases. Our XAFS analyses also indicate that both guest metal species are present in a sulfur-rich environment in their oxidized forms in the material. We believe this suggests that ion exchange is the mechanism of ion removal by Li_xMoS_2, under our conditions. A comparison of these XAFS results with those for MoS_2 that has been lithiated, exfoliated, and restacked under acidic conditions and stored in an aerobic environment suggests that ion-intercalated MoS_2 compounds are susceptible to oxidation by oxygen. The degree of susceptibility of each M_xMoS_2 compound seems to depend on the identity of the intercalated ion. It appears that the soft-heavy-metal-ion-intercalated materials are resistant to oxidation under atmospheric conditions.

Experimental Section

Preparation of $Li_{1.3}MoS_2$ and M_xMoS_2 ($M = Hg^{2+}$, Ag^+) Samples. The black compound $Li_{1.3}MoS_2$ was prepared using a literature procedure.[33] Metal-intercalated solids for our studies were prepared and their levels of intercalation determined in accordance with our previous report.[19]

XAFS Data Acquisition and Analysis. Several of the intercalated compounds were analyzed by XAFS methods, studying both the guest metal ion (Ag or Hg) and the host metal (Mo) of the respective metal chalcogenide. All of the compounds used were sieved fine powders to ensure a uniform sample distribution. For concentrated samples, appropriate amounts were mixed with polystyrene beads (used as an inert, low-Z diluent) to give an edge jump of ≈1 across the Mo K, Ag K, or the Hg L_{III} absorption edges. The compounds were combined with sufficient polystyrene beads to ensure that the mixture could be packed into a 5 × 20 mm slot in an aluminum sample holder (1-mm thick). Samples with dilute metal ion concentrations were prepared without dilution. Kapton tape was used to seal the sample holder and provide an X-ray transparent window. Samples of the reference compounds HgS (cinnabar, red), Hg_2Cl_2, $HgCl_2$, $Hg(OOCCH_3)_2$, Ag_2S (acanthite), and MoS_2 were prepared in an analogous manner.

All spectra were acquired at room temperature in either transmission or fluorescence detection modes (Ge array detector used on dilute Hg and Ag samples) at the Stanford Synchrotron Radiation Laboratory (SSRL) on wiggler beamline 4-1 (unfocused) using a Si(220) double-crystal monochromator. Harmonic rejection was achieved by detuning the monochromator by 50% relative to the maximum incoming flux. The data were calibrated by simultaneously measuring the spectra for Mo foil, Ag foil, or $HgCl_2$ defining the first inflection points at 20 003.9, 25 515.0, and 12 285 eV, respectively.

EXAFS and XANES data reduction was performed by standard methods described elsewhere using the suite of programs EXAFSPAK developed by G. George of SSRL.[34] Data reduction included pre-edge background subtraction followed by spline fitting and normalization (based on the Victoreen falloff) to extract the EXAFS data above the Mo, Ag, and Hg threshold energies, E_0, defined at 20 020, 25 535, and 12 305 eV, respectively. Curve-fitting analyses were performed using EXAFSPAK to fit the raw k^3-weighted EXAFS data. The theoretical EXAFS modeling code, FEFF7, of Rehr et al. was used to calculate the backscattering phases and amplitudes of the different neighboring atoms that were included in the fits.[35] All the fits included single scattering interactions calculated from previously published X-ray diffraction data for the model compounds MoS_2,[34] HgS,[36] $HgCl_2$,[37] Hg_2Cl_2,[38] $Hg(OOCCH_3)_2$,[39] Ag_2S,[40] and Ag metal (face-centered cubic, a = 4.0862 Å). In the case of Hg_2Cl_2, multiple scattering paths (3- and 4-legged linear paths at 4.97 Å associated with the −Hg−Hg−Cl unit) were included and linked directly to the Cl and Hg shells as dependent variables. All fits were done over the full range of k-space data displayed for each sample (see figures below). Note that where possible, the Fourier transforms (FTs) were taken over the following ranges to facilitate accurate comparisons of spectra within a given elemental series: (Hg spectra, $k = 2-12$ Å^{-1}; Ag spectra, $k = 2-10$ Å^{-1}; Mo spectra, $k = 2-14$ Å^{-1}). As a result, the FTs for Hg_2Cl_2 and Ag metal were limited to a $k_{max} = 12$ Å^{-1} while the FT for $Hg(OOCCH_3)_2$ was taken only out to $k = 11$ Å^{-1}. The S_0^2 values are noted in the curve-fitting tables for the Hg, Ag, and Mo spectra. These numbers were obtained by fitting EXAFS data for the model compounds HgS, Ag metal, and MoS_2 and fixing the coordination numbers of the various shells to previously determined crystallographic values.

Results and Discussion

XAFS Analyses of M_xMoS_2 ($M = Ag^+$, Hg^{2+}) Compounds. The goals of the XAFS studies performed on the inclusion compounds reported here were severalfold. XAFS analyses provide information about both the oxidation state and coordination environment of the guest (heavy metals) and the host (Mo). The oxidation state of the guest should address whether the heavy-metal ion has been reduced by the solid $Li_{1.3}MoS_2$. The coordination environments of the guest metals provide evidence of whether cation removal is accompanied by counterion adsorption into the solid. The counterion in this study was nitrate, and EXAFS should be able to differentiate between an oxygen atom and a sulfur atom environment (the anticipated metal-ion environment if the MoS_2 layers are negatively charged).

It is important to note a difference between our intercalation compound preparation procedure and those used by other investigators. Previous studies employed the reaction shown in (1) under initially neutral pH conditions.[3,4,8,24,25] Exfoliation of Li_xMoS_2 is accompanied by the production of hydroxide ions, which could precipitate additional guest metal ions as the metal hydroxide salt. As this process would serve only to make our earlier remediation and subsequent XAFS studies more difficult, we performed our initial syntheses under acidic (pH = 1) conditions. Even after exfoliation/flocculation (production of hydroxide ions), the pH was still acidic (pH ∼ 1.3). This eliminates the precipitation of metal hydroxide as a possible mechanism of ion removal from solution. Furthermore, we believed that eliminating those ion-pair complications would likely yield some information about the role that the each phase, 1T- or 2H-, plays in the inclusion chemistry of MoS_2.

Guest Species XAFS. Figure 1 shows the Hg L_{III} edge XANES spectra for $Hg_{0.02}MoS_2$ (heat-treated $Hg_{0.32}$-

(33) Dines, M. B. *Mater. Res. Bull.* **1975**, *10*, 287.
(34) Prins, R.; Koninsberger, D. E. *X-ray Asborption: Principles, Applications, Techniques for EXAFS, SEXAFS, and XANES*; Wiley-Interscience: New York, 1988.
(35) Rehr, J. J.; Mustre de Leon, J.; Zabinsky, S.; Albers, R. C. *Phys. Rev. B* **1991**, *44*, 4146.
(36) Aurivillius, K. L. *Acta Chem. Scand.* **1950**, *4*, 1413.
(37) Subramanian, V.; Seff, K. *Acta Crystallogr.* **1980**, *B36*, 2132.
(38) Calos, N. J.; Kennard, C. H. L.; Davis, R. L. *Z. Kristallogr.* **1989**, *187*, 305.
(39) Allman, V. R. *Z. Kristallogr.* **1973**, *138*, 366.
(40) Frueh, A. J., Jr. *Z. Kristallogr.* **1958**, *110*, 136.

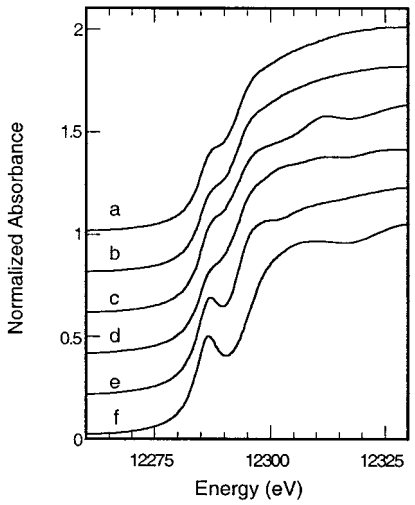

Figure 1. Hg L_{III} edge XANES for (a) $Hg_{0.02}MoS_2$ (heat-treated $Hg_{0.32}MoS_2$), (b) $Hg_{0.32}MoS_2$, (c) HgS (cinnabar), (d) Hg_2Cl_2, (e) $HgCl_2$, and (f) $Hg(OOCCH_3)_2$.

MoS_2), $Hg_{0.32}MoS_2$, HgS (cinnabar), Hg_2Cl_2, $HgCl_2$, and $Hg(CH_3COO)_2$. The last four compounds listed above were used as structural models of the possible oxidation state(s) and coordination environment(s) of mercury in the compounds $Hg_{0.32}MoS_2$ and $Hg_{0.02}MoS_2$. The Hg L_{III} edge has typically been assigned to a $2p_{3/2} \rightarrow 5d$ transition, and the pre-edge feature occurring at ≈12 290 eV has been assigned previously to a $2p \rightarrow 6s$ resonance. Because Hg(I) or Hg(II) ions each have filled 5d states, the main absorption edge is relatively insensitive to these effective charge differences. In contrast, the intensity of the Hg L_{III} pre-edge transition should be sensitive to 6s orbital occupancy. Accordingly, a true Hg(II) species, being $6s^0$, should show a more prominent pre-edge transition than a pure Hg(I) species having a $6s^1$ configuration. The intensity of the pre-edge transition is also dependent on geometry and bond lengths for ions having the same formal valence.[41] As the first-shell bond lengths increase, the intensity of this feature decreases. For example, going from $Hg(CH_3COO)_2$ (2O at 2.07 Å) to $HgCl_2$ (2Cl at 2.28 Å) to HgS (2S at 2.36 Å), the pre-edge amplitudes are observed to decrease for these nominally divalent species. Another method used to quantify the bonding and charge in Hg L_{III} XANES spectra consists of measuring the separation of the first-derivative maxima that correspond to the positive inflection points occurring before and after the pre-edge peak.[42,43] The observation is that larger separations of these features correspond to higher levels of ionic-bonding character. Table 1 shows these derivative results for the spectra in Figure 1.

Using these formalisms, two trends are readily obvious. First, the XANES spectra of both $Hg_{0.32}MoS_2$ and $Hg_{0.02}MoS_2$ appear to most closely match the XANES spectra of both the HgS and the Hg_2Cl_2 model compounds (Figure 1c,d) both in pre-edge intensity and first-derivative separations. Second, the 6s orbital occupancy

Table 1. First-Derivative Inflection Point Energies (eV) from Hg L_{III} Edge XANES Spectra

sample	max. 1	max. 2	difference
Hg_xMoS_2, $x = 0.02$	12 284.9	12 293.2	8.3
Hg_xMoS_2, $x = 0.32$	12 284.9	12 293.2	8.3
HgS (cinnabar, red)	12 285.1	12 293.0	7.9
Hg_2Cl_2	12 284.8	12 293.1	8.3
$HgCl_2$	12 284.6	12 293.4	8.8
$Hg(CH_3COO)_2$	12 284.6	12 295.4	10.8

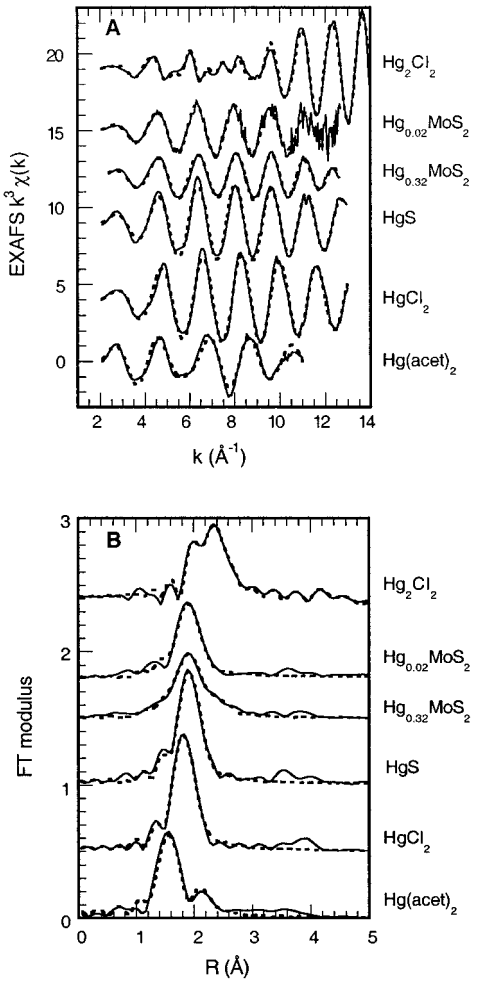

Figure 2. Hg L_{III} edge EXAFS data (A) and corresponding Fourier transforms (B) for the compounds: Hg_2Cl_2, $Hg_{0.02}MoS_2$ (heat-treated $Hg_{0.32}MoS_2$), $Hg_{0.32}MoS_2$, HgS (cinnabar), $HgCl_2$, and $Hg(OOCCH_3)_2$: experimental data (−); theoretical fit (···).

(peak height) and bond covalency (first-derivative separations) for Hg in HgS (formally Hg(II)) closely match those of Hg in Hg_2Cl_2 (formally Hg(I)). This latter point illustrates that the XANES spectra are sensitive to effective charge and bonding rather than formal valence. In this regard, the XANES results indicate that the Hg present in $Hg_{0.32}MoS_2$ has an effective charge and 6s bond character similar to that of the Hg atoms in HgS or Hg_2Cl_2.

The Hg L_{III} edge EXAFS and corresponding Fourier transforms of the compounds $Hg_{0.02}MoS_2$ (heat-treated $Hg_{0.32}MoS_2$), $Hg_{0.32}MoS_2$, Hg_2Cl_2, HgS, $HgCl_2$, and $Hg(CH_3COO)_2$ are shown in Figure 2. The bond lengths (R), coordination numbers (N), Debye−Waller terms (σ^2), and ΔE_0 values for both the model and mercury-included compounds are given in Table 2. EXAFS curve

(41) Åkesson, R.; Persson, I.; Sandstrom, M.; Wahlgren, U. *Inorg. Chem.* **1994**, *33*, 3715.
(42) Huggins, F. E.; Huffman, G. P.; Dunham, G. E.; Senior, C. L. *Energy Fuels* **1999**, *13*, 114.
(43) Huggins, F. E.; Huffman, G. P.; Yap, N., unpublished data compilation.

Table 2. Hg_xMoS_2 EXAFS Curve-Fitting Results[a]

	Hg−O			Hg−X (X = S, Cl)			Hg−Hg			
sample	R (Å)	N	σ^2 (Å^2)	R (Å)	N	σ^2 (Å^2)	R (Å)	N	σ^2 (Å^2)	ΔE_0
$Hg(acet)_2$	2.07	2	0.0030							−6.5
	[2.07]	2								
$HgCl_2$				2.29	2	0.0029				−14.8
				[2.28]	2					
Hg_2Cl_2				2.42	1	0.0035	2.55	1	0.0022	−14.4
				[2.36]	1		[2.59]	1		
HgS (cinnabar, red)				2.38	2	0.0034				−13.0
				[2.36]	2					
HgS (metacinnabar)				[2.54]	4					
Hg_xMoS_2, $x = 0.02$				2.38	1.9	0.0047				−15.0
Hg_xMoS_2, $x = 0.32$				2.37	1.5	0.0048	2.56	0.2	0.0024	−14.6

[a] The coordination number N was held constant for the model compounds using an amplitude reduction factor, $S_0^2 = 0.85$, determined from the HgS fit. The errors in R, N, and σ^2 (95% confidence limits) as estimated by EXAFSPAK are as follows: Hg−O, $R \pm 0.01$ Å, $\sigma^2 \pm 0.0012$ Å^2; Hg−X, $R \pm 0.01$ Å, $N \pm 25\%$, $\sigma^2 \pm 0.0021$ Å^2; Hg−Hg, $R \pm 0.01$ Å, $N \pm 35\%$, $\sigma^2 \pm 0.0021$ Å^2. Entries with square brackets [ ] denote average structural parameters taken from previous X-ray diffraction work noted in the text.

fits to the model compounds are consistent with the published crystal structures noted earlier. The EXAFS curve fits to $Hg_{0.32}MoS_2$ gave a first-shell coordination environment of ≈2 S atoms located at 2.38 Å. Although the amount of disorder is greater (larger σ^2), the observation of S at 2.38 Å is consistent with the type of Hg−S bonding found in HgS (cinnabar). The curve fits for $Hg_{0.32}MoS_2$ also revealed a percentage of Hg−Hg interactions ($N = 0.2 \pm 0.07$) at 2.56 Å. Although the uncertainty in N_{Hg} is large, the Hg−Hg interaction was easily identified in the fits due to its substantially different phase and amplitude relative to Hg−S interactions (note the high-k amplitude in the Hg_2Cl_2 EXAFS due to Hg−Hg scattering). Because EXAFS sees an average of all species present, it is likely that the Hg present in $Hg_{0.32}MoS_2$ was present as a mixture of both HgS-like species and Hg_2^{2+} ions.

This interpretation of our results would indicate that some Hg^{2+} species were reduced to Hg_2^{2+} during the exfoliation/flocculation process; however, the process of exfoliation/flocculation alone is insufficient to produce elemental Hg. Assuming this is true, it is likely that the mercuric species were reduced in part by the solid extractant, $Li_{1.3}MoS_2$. This was not unexpected, as the reduction potential for Hg^{2+} to Hg_2^{2+} is a very positive value of +0.91 V (vs NHE).[44] In addition, we have observed the reduction of $[AuCl_4]^-$(aq) (reduction potential +1.002 V (vs NHE))[44] to Au^0 upon its contact with $Li_{1.3}MoS_2$ under aqueous acidic conditions. Although the EXAFS analyses indicate some reduction of the Hg^{2+} species to Hg_2^{2+}, they also indicate that the mercury present in $Hg_{0.32}MoS_2$ is present as ionic species. If the mercury in $Hg_{0.32}MoS_2$ were entirely present as reduced Hg^0 or Hg(I) species, the EXAFS analyses would certainly have detected a large contribution from Hg−Hg interactions, which was not the case.

It is clear that the EXAFS fitting results for $Hg_{0.32}MoS_2$ describe the majority of mercury present as an ionic form in a sulfur environment. If the mercury atoms in $Hg_{0.32}MoS_2$ were present as intercalated $Hg(NO_3)_2$ species, the mercury would have oxygen in its coordination environment (since NO_3^- was the anion present in solution). This was not observed in the EXAFS analyses of $Hg_{0.32}MoS_2$. These results indicate that the ionic mercury species, either Hg^{2+} or Hg_2^{2+}, in $Hg_{0.32}MoS_2$ is present without charge-compensating nitrate ions. Clearly, there must be charge neutrality in the $Hg_{0.32}MoS_2$ material; therefore, the ionic mercury species present must be there to compensate negatively charged MoS_2 layers.

We have demonstrated that heat treatment of $Hg_{0.32}MoS_2$ (to 350 °C) under vacuum or inert atmosphere conditions, which resulted in the formation of near stoichiometric amounts of elemental mercury and pristine mercury-free 2H−MoS_2.[19] The EXAFS results presented here suggest that the elemental mercury recovered during heating of $Hg_{0.32}MoS_2$ was most likely formed during the heating step and not during the exfoliation/flocculation steps because only Hg^{2+} or Hg_2^{2+} could be identified in the solid before heating. We believe that the heat-treatment process induces an entropy-driven internal redox reaction where the negatively charged $[MoS_2]^{n-}$ layers reduce the intercalated ionic mercury species to elemental mercury that, under high-temperature conditions, volatilizes and is collected separately. Curtis and co-workers have postulated a similar internal redox reaction in the heat treatment of cobaltacenium-intercalated MoS_2.[4]

According to elemental analyses, a small amount of mercury remains in the heat-treated sample, $Hg_{0.02}MoS_2$.[19] On the basis of the XANES and EXAFS results on the heat-treated solid ($Hg_{0.02}MoS_2$), the mercury remaining in the solid is likely to be in the form of HgS (see Table 2 for comparison to HgS). This could have been produced from the decomposition of a small amount of the material during either the heat treatment or extraction processes. Thus, we expect to find only a small contribution to the EXAFS by any mercury, Hg^{2+} in particular, and we also expect to find no Hg−Hg interactions as there are none in HgS.

Figure 3 shows Ag K edge XANES spectra for Ag foil standard, heat-treated $Ag_{0.61}MoS_2$, $Ag_{0.61}MoS_2$, and Ag_2S. The positions of the edge jumps for all four compounds are very similar, making it difficult to assign different oxidation states of the Ag absorber in each compound. In addition, the K-edge absorption edge (1s → 5p) may exhibit a level of insensitivity in terms of measuring charge differences for the species Ag^+ and Ag^0 due to the invariant 5p character in their ground-state electron configurations ($4d^{10}5s^0$ and $4d^{10}5s^1$, respectively). Given this, these spectra appear to be more

(44) Bard, A. J.; Parsons, R.; Jordan, J. *Standard Potentials in Aqueous Solution*; Dekker: New York, 1985.

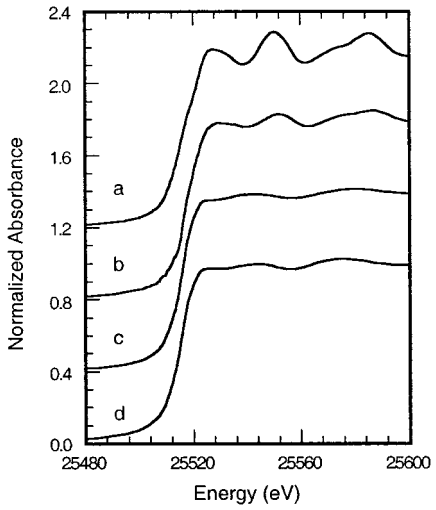

Figure 3. Ag K edge XANES spectra for (a) Ag foil standard, (b) heat-treated $Ag_{0.61}MoS_2$, (c) $Ag_{0.61}MoS_2$, and (d) Ag_2S.

sensitive to real structural differences, attributed to either multiple scattering or the onset of single-scattering EXAFS features displayed here. Indeed, the postedge shape of the spectra for both the Ag foil and the heat-treated $Ag_{0.61}MoS_2$ (Figure 3a,b) are very similar. They are also noticeably different from the data for $Ag_{0.61}MoS_2$ and Ag_2S (Figure 3c,d), yet the shapes of the latter two edge spectra resemble one another. This implies that the coordination environments of the Ag foil and heat-treated $Ag_{0.61}MoS_2$ are similar, as are those of Ag_2S and $Ag_{0.61}MoS_2$. These observations follow with the contention that the silver ions present in $Ag_{0.61}MoS_2$ are present in a sulfur-rich environment (likely not very different from Ag^+ in Ag_2S) while heat treatment of $Ag_{0.61}MoS_2$ leads to the formation of Ag−Ag interactions. This latter point implies the formation of silver crystallites in the heat-treated $Ag_{0.61}MoS_2$ sample.

The Ag K edge EXAFS data and corresponding Fourier transforms of the Ag foil standard, heat-treated $Ag_{0.61}MoS_2$, $Ag_{0.61}MoS_2$, and Ag_2S are presented in Figure 4 and the results of the curve-fitting analyses are shown in Table 3. These results confirm the assignments made from the XANES spectra. In particular, one can see that the environment of the silver ion in $Ag_{0.61}MoS_2$ is sulfur-rich with two S atoms coordinated to the silver ion at a distance of 2.43 Å. These parameters are similar to those observed for the compound Ag_2S. In addition, curve fits detected a shell of heavier atoms located at 2.9 Å. This shell was best fit with Ag−Ag interactions, although it is possible that it could also be attributed to Mo next nearest neighbors. The presence of either of these interactions (or a combination of the two) is plausible for this intercalated compound.

The coordination environment of silver in heat-treated $Ag_{0.61}MoS_2$ is quite different when compared to that in $Ag_{0.61}MoS_2$. The scattering amplitude of the heat-treated sample, as shown in Figure 4, strongly resembles that of elemental silver. Preliminary curve fits to this spectra confirmed the presence of Ag−Ag interactions consistent with a fcc lattice and also revealed a fraction of Ag−S interactions. (Powder XRD analysis of heat-treated $Ag_{0.61}MoS_2$ indicated a small amount of Ag_2S.) As a result, final curve fits included both Ag−S and Ag−Ag interactions, the latter of which were constrained in

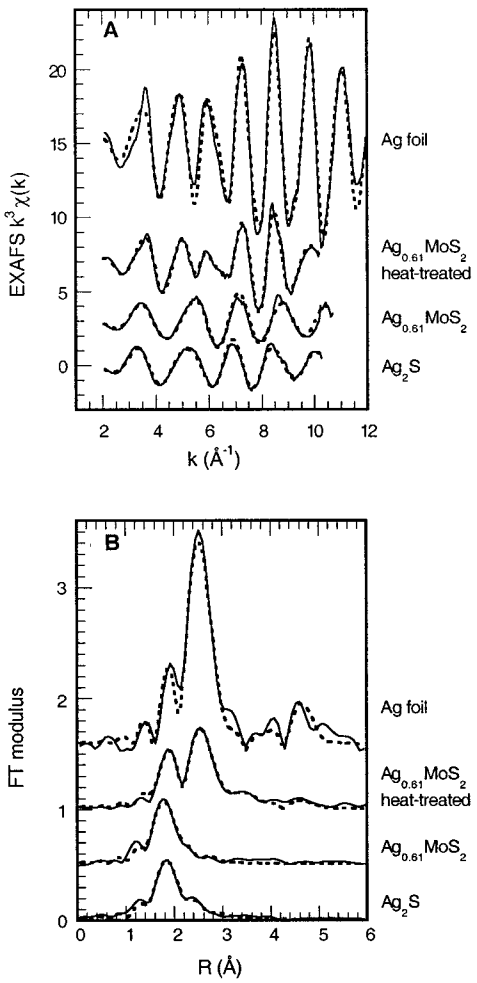

Figure 4. Ag K edge EXAFS data (A) and corresponding Fourier transforms (B) for the compounds: Ag foil, heat-treated $Ag_{0.61}MoS_2$, $Ag_{0.61}MoS_2$ (1.5×), and Ag_2S (1.5×): experimental data (−); theoretical fit (···).

Table 3. Ag EXAFS Curve-Fitting Results[a]

	Ag−S			Ag−Ag			
sample	R (Å)	N	σ^2 (Å^2)	R (Å)	N	σ^2 (Å^2)	ΔE_0
Ag_2S	2.52	1.7	0.0071	3.00	1	0.0137	−14.4
	[2.52]	1.7		[3.04]	1		
	2.74	1.3	0.0184				
	[2.81]	1.3					
Ag_xMoS_2, $x = 0.61$	2.43	1.6	0.0073	2.91	1.3	0.0200	−18.9
Ag_xMoS_2, $x = 0.61$	2.49	0.9	0.0050	2.86	5.9[b]	0.0118	−17.4
(heat-treated)				4.01	2.9[b]	0.0081	
				4.96	11.8[b]	0.0220	
Ag metal (EXAFS)				2.86	12	0.0096	−18.2
				[2.88]	12		
				4.02	6	0.0140	
				[4.08]	6		
				5.00	24	0.0150	
				[5.00]	24		

[a] The coordination number N was held constant for the model compounds using an amplitude reduction factor, $S_0^2 = 0.85$, determined from the Ag metal fit. The errors for R, N, and σ^2 (95% confidence limits) as estimated by EXAFSPAK are as follows: Ag−S, $R \pm 0.01$ Å, $N \pm 17\%$, $\sigma^2 \pm 0.0012$ Å^2; Ag−Ag, $R \pm 0.03$ Å, $N \pm 36\%$, $\sigma^2 \pm 0.0032$ Å^2. Entries with square brackets [ ] denote average structural parameters taken from previous X-ray diffraction work noted in the text. [b] Coordination numbers for the Ag−Ag shells were constrained at a ratio of 2:1:4.

accord with Ag−Ag coordination number ratios from Ag metal. The decreased Ag−Ag coordination numbers relative to Ag metal are consistent with the formation

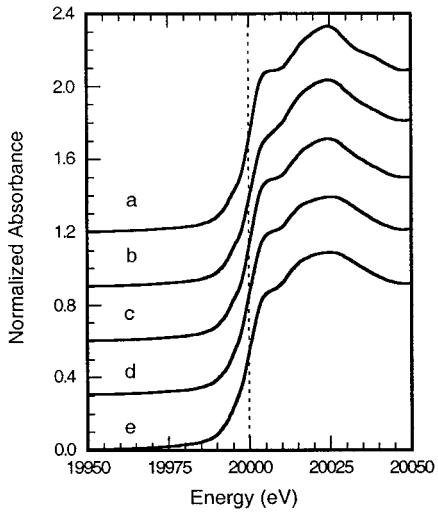

Figure 5. Mo K edge XANES spectra for (a) native MoS_2, (b) $Hg_{0.02}MoS_2$ (heat-treated $Hg_{0.32}MoS_2$), (c) $Li_{0.10}H_{0.78}MoS_2$ ($Li_{1.3}MoS_2$ exfoliated and restacked in 0.1 M HNO_3, (d) $Li_{1.3}MoS_2$, and (e) $Hg_{0.32}MoS_2$.

of a percentage of elemental silver clusters along with a fraction of Ag_2S. The Ag_2S was likely formed during either the heat treatment or extraction processes. Transmission electron microscopic (TEM) studies have been performed to confirm these results and will be reported elsewhere.[45] Nonetheless, the Ag EXAFS results show clear evidence for the reduction of intercalated Ag^+ ions to Ag^0 when $Ag_{0.61}MoS_2$ is heated to 500 °C. Just as with the $Hg_{0.32}MoS_2$ sample, we believe that the heat treatment of the solid $Ag_{0.61}MoS_2$ leads to an internal redox reaction where the negatively charged MoS_2 layers reduce the intercalated Ag^+ ions to Ag^0.

Host Mo XAFS. In addition to studying the XAFS characteristics of the guest metal ions, we studied the local environment of the host Mo species. Figure 5 shows the Mo K edge XANES spectra for MoS_2, $Hg_{0.02}MoS_2$, $Li_{0.10}H_{0.78}MoS_2$ ($Li_{1.3}MoS_2$ exfoliated and restacked in 0.1 M HNO_3), $Li_{1.3}MoS_2$, and $Hg_{0.32}MoS_2$ samples. (The stoichiometry of the compound $Li_{0.10}H_{0.78}MoS_2$ was determined through mass balance experiments.)[45] The shape and position of Mo K absorption edges for all of the analyzed samples closely match that of native MoS_2. This was initially surprising because the average formal oxidation state of the Mo atoms in these samples varies from +2.7 to +4.0 (as inferred from the quantity of intercalated cations). However, previous studies of $M_{0.5}(OH)_x(H_2O)MoS_2$ compounds have shown that a negative charge on the MoS_2 layers (indicated by a shift in the absorption edge energy toward lower values) was more clearly demonstrated using S K edge XANES than using Mo K edge XANES.[24]

Closer inspections of the Mo EXAFS spectra (Figure 6A) show what appears to be a loss of spectral features in samples where significant amounts of either lithium ion or mercuric ion were present. The EXAFS spectra for MoS_2, $Hg_{0.02}MoS_2$, and $Li_{0.10}H_{0.72}MoS_2$ all have a more complex beat pattern as observed around $k = 4$ Å^{-1} and $k = 10-12$ Å^{-1}. This structure is not present in the EXAFS spectra of $Li_{1.3}MoS_2$, $Hg_{0.32}MoS_2$, or $Ag_{0.61}MoS_2$. At this level of analysis, the loss of this structure in the latter spectra suggests that a shell of neighboring atoms has been removed, relative to MoS_2, for these compounds.

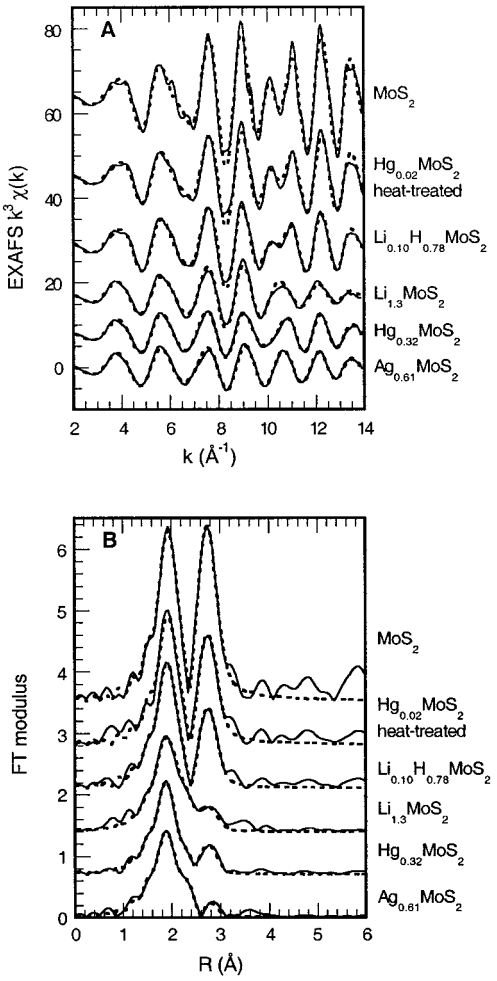

Figure 6. Mo K edge EXAFS data (A) and corresponding Fourier transforms (B) for MoS_2 (Aldrich), $Hg_{0.02}MoS_2$ (heat-treated $Hg_{0.32}MoS_2$), $Li_{0.10}H_{0.78}MoS_2$ ($Li_{1.3}MoS_2$ that has been exfoliated and flocculated in 0.1 M HNO_3, made under aerobic conditions), $Li_{1.3}MoS_2$, $Hg_{0.32}MoS_2$ (made under aerobic conditions), and $Ag_{0.61}MoS_2$ (aerobic conditions): experimental data (−); theoretical fit (···).

The Mo K edge EXAFS Fourier transforms for the compounds MoS_2, $Hg_{0.02}MoS_2$, $Li_{0.10}H_{0.78}MoS_2$, $Li_{1.3}MoS_2$, $Hg_{0.32}MoS_2$, and $Ag_{0.61}MoS_2$ are shown in Figure 6B, and the corresponding curve fit results are given in Table 4. The results for native MoS_2 are consistent with the crystal structure that has six Mo−S bonds at 2.42 Å in a trigonal prismatic arrangement and six Mo−Mo interactions at a distance of 3.16 Å.[46] For all of the intercalated samples, the Fourier transforms and curve fits indicate that the first-shell Mo−S coordination is retained. Although the first-shell Mo−S peak positions are the same for all of the compounds, the first-shell peaks for $Li_{1.3}MoS_2$, $Hg_{0.32}MoS_2$, and $Ag_{0.61}MoS_2$ are broader with diminished amplitude relative to those for the other three compounds. One might expect this to signify a larger range of Mo−S distances or increased disorder, which is confirmed by the larger Debye−

(45) Gash, A. E.; Dysleski, L. M.; Flashenriem, C. J.; Dorhout, P. K.; Strauss, S. H., in preparation.

(46) Dickinson, R. G.; Pauling, L. *J. Am. Chem. Soc.* **1923**, *45*, 1466.

Table 4. Mo EXAFS Curve-Fitting Results[a]

	Mo−S			Mo−Mo			
sample	R (Å)	N	σ^2 (Å^2)	R (Å)	N	σ^2 (Å^2)	ΔE_0
MoS_2	2.41	6	0.0026	3.17	6	0.0036	−17.9
	[2.42]	6		[3.17]	6		
Hg_xMoS_2, $x = 0.02$	2.41	5.2	0.0034	3.17	4.4	0.0043	−17.0
$Li_xH_yMoS_2$, $x < 0.1$	2.41	5.4	0.0039	3.18	3.9	0.0053	−17.3
Li_xMoS_2, $x = 1.3$	2.42	4.8	0.0046	3.17	1.8	0.0067	−18.7
				2.78	0.8	0.0038	
Hg_xMoS_2, $x = 0.32$	2.41	4.7	0.0045	3.18	1.3	0.0050	−20
				2.68	0.9	0.0080	
Ag_xMoS_2, $x = 0.61$	2.42	4.9	0.0055	3.17	1.1	0.0076	−19
				2.71	1.0	0.0052	
Ag_xMoS_2(HT), $x = 0.61$	2.41	5.2	0.0032	3.17	4.5	0.0047	−17

[a] The coordination number N was held constant for the model compounds using an amplitude reduction factor, $S_0^2 = 0.94$, determined from the MoS_2 fit. The standard deviations (1σ) for R, N, and σ^2 estimated by EXAFSPAK are as follows: Mo−S, $R \pm 0.004$ Å, $N \pm 6\%$, $\sigma^2 \pm 0.0005$ Å^2; Mo−Mo, $R \pm 0.006$ Å, $N \pm 36\%$, $\sigma^2 \pm 0.0016$ Å^2. Entries with square brackets [ ] denote average structural parameters taken from previous X-ray diffraction work noted in the text.

Waller factors obtained in the curve fits relative to native MoS_2. A plausible explanation would be that it is due to static disorder whereby Mo atoms in the compounds $Li_{1.3}MoS_2$, $Hg_{0.32}MoS_2$, and $Ag_{0.61}MoS_2$ are present in more than one coordination environment.

All of the samples analyzed displayed peaks associated with the Mo−Mo absorber−scatterer pairs that were less intense than the 3.16 Å Mo−Mo interaction for native MoS_2. In addition, the Mo−Mo peaks for $Li_{1.3}MoS_2$, $Hg_{0.32}MoS_2$, and $Ag_{0.61}MoS_2$ are much weaker than those are for $Li_{0.10}H_{0.78}MoS_2$ and $Hg_{0.02}MoS_2$. This indicates that in the former three cases the second shell of Mo atoms has been disturbed. Indeed, curve fits show decreased N_{Mo} (3.17 Å) values of 1.8, 1.3, and 1.1 for $Li_{1.3}MoS_2$, $Hg_{0.32}MoS_2$, and $Ag_{0.61}MoS_2$, respectively, and a new shell of Mo atoms at ≈2.7 Å. The partial loss of the 3.17-Å Mo−Mo interaction and the appearance of a new one at ≈2.7 Å may result from a change in site symmetry and/or a phase change. Similar EXAFS results have been attributed to the phase change in MoS_6 coordination from trigonal prismatic (2H) to distorted octahedral (1T) for single layers of exfoliated and restacked MoS_2 as well as solid compounds such as $M_{0.5}(OH)_x(H_2O)MoS_2$.[4,24,25] Therefore, we conclude that the MoS_2 layers in $Li_{1.3}MoS_2$, $Hg_{0.32}MoS_2$, and $Ag_{0.61}MoS_2$ are present as a mixture of the 1T- and 2H-phases. The presence of Hg^{2+} or Ag^+ ions in the compounds $Hg_{0.32}MoS_2$ or $Ag_{0.61}MoS_2$ may serve to stabilize the distorted octahedral MoS_6 coordination units within the 1T-phase $[MoS_2]^{n-}$ layers.

From mass balance studies, it has been confirmed that MoS_2 that has been lithiated, exfoliated, and restacked in 0.1 M HNO_3 should be regarded as $Li_{0.10}H_{0.78}MoS_2$.[45] This material has intercalated cations; however, EXAFS results do not detect a significant fraction (<15%) of the 1T-phase (lack of 2.7-Å interactions), as we have observed in the cases with M_xMoS_2 ($M = Li^+$, Ag^+, Hg^{2+}). This compound was made under aerobic conditions and stored in air until the XAFS analyses were performed (≈2 weeks); therefore, the host layers could have been oxidized by water or oxygen during that time period. The Hg^{2+} and Ag^+ included compounds were prepared and stored identically and yet they still retain a significant degree of the 1T-phase in their EXAFS Fourier transforms. These seemingly contradictory observations may be due to the fact that each included ion affords a different degree of stabilization to the reduced MoS_2 layers. The chalcophilic mercuric and silver ions are quite likely to be very stabilizing to reduced sulfide layers. However, the mixture of protons and lithium ions (both considered hard cations by Pearson's Hard Soft Acid Base principle)[47] that are present in the exfoliated and restacked material likely do not stabilize the negative charge on the sulfide layers very well. Therefore, it is possible that the material is more susceptible to oxidation than the heavy-metal-ion-intercalated compounds. This potential hypothesis can also be used to rationalize some of the previous contradictions in the literature concerning the Mo EXAFS of metal-included MoS_2 compounds. This hypothesis relies on the key assumption that the 1T-phase of MoS_2 is only observed for reduced (i.e., negatively charged) MoS_2 and the 2H-phase is present when the MoS_2 layers are fully oxidized (i.e., neutral).

Zubavichus et al. reported the presence of the 1T-phase of MoS_2 in the Ru^{2+} and Ni^{2+} included compounds; however, no trace of that phase was seen in the Mn^{2+} and Co^{2+} included materials.[24,25] No details were reported of the materials handling or the age of the samples when XFAS data were collected. It appears that the more chalcophilic ions (Ru^{2+}, Ni^{2+}) were more stabilizing toward the inclusion compound; thus, the reduced phase was retained. It is possible that the harder metal ions (Co^{2+}, Mn^{2+}) did not stabilize the negative charge on the layers and the layers were likely oxidized to neutral 2H−MoS_2 upon exposure to oxygen or water. It is not known if the oxidation of the $M_{0.5}(OH)_x(H_2O)MoS_2$ is caused by oxygen or intercalated water. Its potential self-oxidation by the intercalated water molecules is shown in eq 2. The MoS_2 layers could be slowly oxidized by water to form hydroxide ion and

$$M_{0.5}(OH)_x(H_2O)_yMoS_2(s) \rightarrow M_{0.5}(OH)_{x+z}(H_2O)_{y-z}MoS_2(s) + z/2H_2(g) \quad (2)$$

hydrogen. The hydroxide ion would stay in the interlayer galleries to maintain charge neutrality in the compound. It is likely that parameters such as ambient temperature, humidity, and the identity of the metal ion would affect the rate of this reaction.

Curtis et al. have reported Co^{2+} included MoS_2 where the Mo EXAFS showed clear evidence of a mixture of both the 1T- and 2H-phases (the reduced and oxidized MoS_2 forms in our hypothesis).[4] The preparation and storage of this material was performed with an effort to minimize the exposure to oxygen and minimize the time between synthesis and XAFS data collection. These same procedures were used in the preparation of exfoliated and restacked MoS_2 whose EXAFS analysis indicated the presence of both the 1T- and 2H-phases (this was not observed in our exfoliated and restacked material, but our preparation and storage conditions were not anaerobic). Therefore, the differences between our results and those of previous studies could be

(47) Pearson, R. G. *Surv. Prog. Chem.* **1969**, *5*, 1−52.

attributed to the handling and storage of the compounds as well as the nature of the intercalated ion.

Conclusions

The Mo XAFS data support the following sequence of structural changes that take place during the preparation of $Hg_{0.32}MoS_2$ and $Ag_{0.61}MoS_2$ from $Li_{1.3}MoS_2$. When lithium ions are intercalated into native MoS_2, under reducing conditions, the host compound undergoes a structural change. The coordination of the Mo atoms partially changes from trigonal prismatic (2H-polymorph) to the metastable octahedral form (1T-polymorph).[48−50] This is the structural change that leads to the observed differences (2.7-Å interaction and reduced 3.16-Å interaction) between the Mo EXAFS of $Li_{1.3}MoS_2$ and that of native molybdenum disulfide. When $Li_{1.3}MoS_2$ is exfoliated and restacked in 0.1 M HNO_3 under aerobic conditions, the Li^+ ions are removed from the interlayer space of the solid and replaced by protons. There appears to be a tendency for the Mo coordination to return to that of native MoS_2 (note the similarity of the EXAFS transforms of $Li_{0.10}H_{0.72}MoS_2$ and native MoS_2). Alternatively, when $Li_{1.3}MoS_2$ is exfoliated and flocculated in 0.1 M HNO_3 in the presence of heavy-metal ions such as Hg^{2+}(aq) or Ag^+(aq), the Mo atoms tend to retain the distorted octahedral coordination present in $Li_{1.3}MoS_2$. This suggests that, under these conditions (pH $\sim$ 1), mercuric and silver ions are able to stabilize the negative charge on the MoS_2 layers. The presence of Li^+(aq) and H^+(aq) ions in the exfoliated/flocculated solid $Li_{0.10}H_{0.72}MoS_2$ is not sufficient to retain the 1T-phase. This implies that different ions have different stabilizing capacities on their $[MoS_2]^{n-}$ hosts under aerobic conditions.

Acknowledgment. This work was done (partially) at SSRL, which is operated by the Department of Energy, Division of Chemical Sciences. Additional EXAFS experimental support was provided by the Actinide Chemistry Group at Lawrence Berkeley National Laboratory. Funding for this program was provided by the U.S. Department of Energy Environmental Management Science Program (DE-FG07-96ER14696 to P.K.D. and S.H.S.).

CM000389P

(48) Chrissafis, K.; Zamani, M.; Kambas, K.; Stoemenos, J.; Economou, N. A. *Mater. Sci. Eng. B* **1989**, *3*, 145.

(49) Ouvard, G. *Host Structures Modifications Induced by Intercalation/Deintercalation Into Lamellar Chalcogenides*; Bernier, P. E. A., Ed.; Plenum Press: New York, 1993; p 1.

(50) Sandre, E.; Brec, R.; Rouxel, J. *J. Solid State Chem.* **1990**, *88*, 269.